

LIMITED ANGLE IMAGE RECONSTRUCTION USING FOUR HIGH RESOLUTION PROJECTION AXES AT CO-PRIME RATIO VIEW ANGLES

Anastasios L. Kesidis

*Computational Intelligence Laboratory, Institute of Informatics and Telecommunications,
National Center for Scientific Research "Demokritos", GR-153 10 Agia Paraskevi, Athens, Greece*

Keywords: Image reconstruction, limited angle tomography, coprime view angles, inverse problems.

Abstract: This paper proposes a sequential image reconstruction algorithm for the exact reconstruction of an image from a limited number of projection angles. Specifically, four projection axes oriented at coprime ratio view angles are used. The set of proper values for the view angles as well as the overall number of samples on the projection axis are explicitly defined and are related only to the dimensions of the image. The slopes of the four projection axes are calculated according to the chosen view angle and are symmetrically oriented with respect to the horizontal and the vertical axis. The reconstruction is a non-iterative, one pass process based on a decomposition sequence which defines the order in which the image pixels are restored. Several simulation results are provided that demonstrate the feasibility of the proposed method.

1 INTRODUCTION

Computerized tomography (CT) is an important and effective tool for a large number of imaging applications allowing the observation of the internal structure of objects. The majority of applications refer to the medical sciences including x-ray tomography, magnetic resonance imaging, electron microscopy tomography, and diagnostic radiology. (CT) is also extensively used in the industry for non-destructive evaluation allowing the determination of defects and abnormalities in industrial objects. In general, the object is reconstructed from the projection data acquired by projecting it into several fairly equidistant view angles. However, there are several cases in which projection data can be acquired only in a limited range of projection view angles. The limited angle tomography problem concerns a wide range of applications in surgical imaging, dental radiology and positron emission mammography as well as in electron microscopy and in astronomy. It is well known that applying the conventional filtered backprojection reconstruction method and assuming zero values for the missing view angles produces approximations of the original image containing significant artefacts (Natterer, 2001). Several approaches have been proposed that

address this problem including sinogram techniques, Bayesian methods, projections onto convex sets, maximum entropy techniques and many others. Recently, Rantala *et al* (Rantala, 2006) addressed the reconstruction from limited angle data by using a wavelet expansion approximation and Besov space a priori information in order to compute a maximum a posteriori estimation for the original image. A pre-thresholding method is also proposed in which thresholding is applied to the wavelet coefficients prior to the computation of the reconstruction. Delaney and Bresler (Delaney, 1998) formulate the reconstruction problem as a regularized weighted least-squares optimization problem, and propose a family of regularization functionals that are meant to apply a constraint of piecewise smoothness on the image. Clackdoyle *et al* (Clackdoyle, 2004) focus on 2-D reconstruction processes where data from entire projection directions are unmeasured or unavailable and state that region-of-interest reconstruction from these truncated projections is possible under certain conditions. Both direct and statistically based (iterative) reconstruction algorithm can be used for the image reconstruction. Schule *et al* (Schule, 2005) describe how multi-valued objects can be reconstructed by combining binary decisions. They use convex-concave regularization to improve the reconstruction quality as well as the EM-algorithm

to motivate the adaption of the absorption coefficients as hidden data estimation.

In this paper we propose a method for exact image reconstruction when a limited number of projections axes (i.e. four) is available that consists of projection samples with higher resolution than the pixels of the reconstructed image. Reconstruction under such conditions may occur in cases where it is very hard to obtain projections; however, it is possible in these projections to use high resolution detectors, or in cases that is not necessary to reconstruct high resolution images. Examples of such cases are in surgical imaging, in imaging nuclear waste sites or in non destructive testing. More specifically, we propose a method that allows the exact reconstruction of an image assuming four projection axes oriented at coprime ratio view angles. The original grayscale image is projected into the four projection axes and the collected projection data are stored in an accumulator array. The set of proper values for the view angle as well as the overall number of samples on the projection axis are related only to the dimensions of the image. The slopes of the four projection axes are calculated according to the chosen view angle and are symmetrically oriented with respect to the horizontal and vertical axes. The reconstruction is a non-iterative, one pass process that uses a decomposition sequence which defines the order in which the image pixels are restored. The decomposition sequence is determined so that, a unique correspondence between a pixel in the exterior of the image and a projection ray that intersects only this pixel, is preserved during the reconstruction process. Initially, the determination of the view angle and the decomposition sequence is based on the pixels in the 1st octant of the image. However, during the reconstruction process, the symmetrical geometric properties of the pixels in the other octants are used in order to restore all the image's pixels.

The rest of this paper is organized as follows: Section 2 presents an initial approach to determine a proper view angle that allows the exact reconstruction of the image. Besides the view angle, certain projection parameters are also defined that determine the geometry of the reconstruction utilization. In section 3 we extend the methodology in order to determine a set of several other coprime ratio view angles that can also be used in the proposed reconstruction scheme. We provide generalized versions of the projection parameters that are related only to the image dimensions and the slope of the projection axis. Time and memory complexity issues are also considered and the

applicability of the proposed method using various projection view angles is also demonstrated. Finally, section 4 draws the conclusion.

2 AN INITIAL APPROACH FOR EXACT IMAGE RECONSTRUCTION

2.1 Accumulator Array

Without loss of generality let us suppose an input image I of size $N \times N$ pixels where N is assumed to be an even positive integer. A pixel in the input image at position (i, j) has grayscale (intensity) value $I(i, j)$, with $i, j = -N/2 \dots N/2 - 1$, and is assumed to be a square area of unit size with constant intensity value. The projection data obtained by projecting the image into K_θ projection axes is stored in an accumulator array C . Each projection axis consists of a finite number of projection rays s_l where $l=1, 2, \dots, K_l$. Clearly, each sample in array $C(\theta, s)$ corresponds to a projection ray identified by the combination of the slope θ_k with the displacement value s_l . If $I_{\theta, s}$ denotes the set of image pixels that a projection ray $r_{\theta, s}$ intersects, then for each pixel $(i, j) \in I_{\theta, s}$ we define the weighting factor $w_{\theta, s}(i, j)$ to be the area of the portion of $r_{\theta, s}$ inside pixel (i, j) . Thus, each sample of C is calculated as

$$C(\theta, s) = \sum_{(i, j) \in I_{\theta, s}} I(i, j) w_{\theta, s}(i, j) \quad (1)$$

2.2 Projection Parameters Determination

The image is divided into 8 octants as shown in Fig. 1 where the gray shaded pixels denote the 1st octant. A pixel (i, j) in the 1st octant has coordinates $0 \leq i \leq N/2 - 1, 0 \leq j \leq i$. The black pixels in Fig. 1 denote pixels in all octants that have symmetrical geometric properties. There are also $K_\theta=4$ projection axes shown at slopes

$$\theta_k = (u, \frac{\pi}{2} - u, \frac{\pi}{2} + u, \pi - u) \quad \text{for } k=1 \dots K_\theta \quad (2)$$

where u is the projection view angle. The following discussion refers to pixels in the 1st octant and will be later generalized for the pixels in all octants based on the symmetrical positioning of the pixels relatively to the image's center.

Let us consider the four instances shown in Fig. 2 as the first steps of a decomposition sequence regarding the pixels in the 1st octant. By convention, the diagonal pixels are attributed to the odd octants. The decomposition sequence refers to pixels in the last column of the 1st octant, namely pixels $(i, i-n)$, where $i=N/2-1$ and $n=0 \dots i$ denotes an positive offset from the diagonal. Our intention is to identify the width of the projection ray as well as its displacement on the projection axis that provide the largest possible intersection area without intersecting any other pixel of the current or the adjacent octant (octants 1 and 2 in this case). Lines r_1 and r_2 are perpendicular to the projection axis and define the boundaries of the projection ray. For each n , the intersection between projection ray $r_{\theta, s}$ and pixel $(N/2-1, N/2-1-n)$ is considered. For all forthcoming values of n , the pixel just examined and its counterpart in the 2nd octant are ignored. Hence, in Fig. 2b pixel (i, i) is ignored, and pixel $(i, i-1)$ is considered. Clearly, any line r_2 further away from the origin does not affect the intersection area. On the other hand, if line r_1 is shifted in parallel towards the origin then pixels $(i-1, i)$ and $(i, i-2)$ are also intersected by projection ray $r_{\theta, s}$ which is undesirable. Again, in the following steps pixel $(i, i-1)$ as well as its counterpart in 2nd octant, pixel $(i-1, i)$, are ignored.

The process is repeated in Figs. 2c and 2d for pixels $(i, i-2)$ and $(i, i-3)$, respectively. As shown in Fig. 2d line r_1 is determined by points p_1 and p_3 and is the closest to the origin line for which the projection ray intersects only pixel $(i, i-n)$. Line r_2 is a line parallel to r_1 that intersects the upper right vertex of pixel $(i, i-n)$, namely point p_2 . It can be noticed that for $n>1$ point p_3 corresponds to the upper right vertex of pixel $(i-1, i-1)$ while points p_1 and p_2 are related to n . Setting $i=N/2-1$ and $n=i$, and based on the geometry of the utilization as shown in Fig. 2d allows the determination of the projection parameters

$$\begin{aligned} u &= \arctan(2/(N-2)), \quad d = 2/\sqrt{N^2 - 4N + 8}, \\ w &= 1/(N-2), \quad K_p = N/2 \quad \text{and} \quad K_l = N^2/2 \end{aligned} \quad (3)$$

where u is the view angle of the projection axis, d denotes the width of each projection ray, w is the area between any pixel and the furthest from the origin projection ray that intersects it, while K_p and K_l denote the number of rays that intersect a pixel and the overall number of samples on the projection axis, respectively. These parameters are related only

to the image dimension N . The weighting factor $w_{\theta, s}(i, j)$ in (1) equals

$$w_{\theta, s}(i, j) = \begin{cases} w & \text{if } \{s = s_c \text{ or } s = s_f\} \\ 2w & \text{otherwise} \end{cases} \quad (4)$$

where s_c and s_f denote the nearest and furthest from the origin projection ray that intersect pixel (i, j) , respectively.

2.3 Image Reconstruction

Let us suppose that the original image is projected onto the four projection axes each one consisting of K_l samples. The overall projection data, i.e. $K_\theta K_l$ samples, are stored in accumulator array C . In the following we present how the original image can be exactly reconstructed from the samples in array C .

Let I_R denote the reconstructed image. In section 2.2 we stated that the main criterion for the determination of the projection parameters is that the furthest from the origin projection ray that intersects a pixel does not intersect the upper right area w of any other pixel in the same octant. Thus for each pixel (i, j) there is a specific sample at slope θ_k and displacement value s_l that corresponds to this projection ray. This sample is used in order to determine the corresponding pixel's grayscale value $I_R(i, j)$. Having obtained its value, the pixel's contribution is removed from the accumulator array i.e., all the samples of C affected by this pixel decrease their value by an amount proportional to the weighting factor $w_{\theta, s}(i, j)$.

The order in which the pixels are examined is given by a decomposition sequence $T_1\{t\}$ initially defined for the pixels in the 1st octant. The sequence $T_1\{t\}$ contains the pixels of the 1st octant sorted column wise from the periphery to the inner of the image, i.e. pixels $(N/2-1, N/2-1)$, $(N/2-1, N/2-2)$, ..., $(N/2-1, 0)$, $(N/2-2, N/2-2)$, $(N/2-2, N/2-3)$, ... etc, down to $(0, 0)$. For each pixel of the decomposition sequence its symmetric counterparts in the other octants are also examined before the decomposition continues with the next sequence element. The reconstruction process starts with the first member of $T_1\{t\}$, pixel $(i, j) = (N/2-1, N/2-1)$. Let $s_f(i, j)$ denote the furthest from the origin projection ray of projection axis θ_1 that intersects pixel (i, j) . For $\hat{\theta} = \theta_1$ and $\hat{s} = s_f(i, j)$ projection ray $r_{\hat{\theta}, \hat{s}}$ intersects only pixel (i, j) . The accumulator array sample $C(\hat{\theta}, \hat{s})$, that holds the value of projection

ray $r_{\hat{\theta},\hat{s}}$, equals the weighted portion $w_{\hat{\theta},\hat{s}}(i,j)$ of pixel's (i,j) grayscale value. Hence, pixel $I_R(i,j)$ in the reconstructed image can be calculated as

$$I_R(i,j) = \frac{C(\hat{\theta},\hat{s})}{w_{\hat{\theta},\hat{s}}(i,j)} \text{ for } \hat{\theta}=\theta_1 \text{ and } \hat{s}=s_f(i,j) \quad (5)$$

After the determination of $I_R(i,j)$ the contribution of pixel (i,j) is removed from the other samples of C . Specifically, if $P_{\theta}(i,j)$ denotes the set of projection rays $r_{\theta,s}$ that intersect pixel (i,j) at any angle θ_k then the accumulator array is updated as follows

$$C(\theta,s) \leftarrow C(\theta,s) - I_R(i,j)w_{\theta,s}(i,j) \quad (6)$$

for $\{(\theta,s) : r_{\theta,s} \in P_{\theta}(i,j)\}$.

So far, we considered pixels in the 1st octant. Applying proper re-indexing allows the manipulation of pixels in all other octants. Thus, before continuing with the next member of $T_1\{t\}$ the above process is applied to pixels in the other octants that are symmetrical to pixel (i,j) . There are four or eight of them depending on whether pixel (i,j) lies on the diagonal axis or not. Thus, if $M_T(i,j)$ denotes the set of pixels that are symmetrical to pixel (i,j) then

$$M_T(i,j) = \begin{cases} \{(i,i),(-i-1,i),(-i-1,-i-1),(i,-i-1)\} & \text{if } i=j \\ \{(i,j),(j,i),(-j-1,i),(-i-1,j),(-i-1,-j-1), \\ (-j-1,-i-1),(j,-i-1),(i,-j-1)\} & \text{if } i \neq j \end{cases} \quad (7)$$

The process continues with the next element of the decomposition sequence until all the pixels in all octants are examined. Finally, the accumulator array becomes empty and the reconstructed image equals the original one, that is, corresponding pixels in I and I_R have identical intensity values.

3 GENERALIZATION FOR RATIONALLY SLOPED PROJECTION AXES

In this section we show that the determination of the decomposition sequence $T_1\{t\}$ by sorting the pixels column-wise from the periphery to the inner of the image is not unique. In fact, it corresponds to a special case of a general set of parameter settings that allow the reconstruction of the image from several other projection axes that are rationally sloped.

3.1 Projection Slope Determination

In the following by *projection line* we mean a line that defines the border between adjacent projection ray, e.g. lines r_1 and r_2 in Fig.2. Also, the term *lattice points* refers to points on the image plane that correspond to the upper right vertex of the pixels in the 1st octant. Let $p_3(a)=(N/2-a, N/2-a)$ be a lattice point corresponding to the upper right vertex of a diagonal pixel with offset a relatively to lattice point $(N/2,N/2)$. Points $p_3(a)$ and $p_1=(N/2,0)$ form a projection line with slope

$$m = \frac{p_{3,y} - p_{1,y}(a)}{p_{3,x} - p_{1,x}(a)} = 1 - \frac{N}{2a} \quad (8)$$

The view angle u of a projection axis perpendicular to m is given by

$$u = \arctan\left(-\frac{1}{m}\right) = \arctan\left(\frac{2a}{N-2a}\right) \quad (9)$$

Since the range of view angles in the 1st octant is $0 \leq u \leq \pi/4$ it follows from (9) that valid integer values for offset a are in the range

$$a \in \{1 \dots \lfloor N/4 \rfloor\} \quad (10)$$

where symbol $\lfloor x \rfloor$ stands for the largest integer less than or equal to x .

Our intention in the selection of a proper slope m (which in turn affects the value of the perpendicular view angle u) is to form a utilization of adjacent projection rays in such a way that the upper right area of each pixel in the 1st octant is intersected by only one projection ray. Reconsidering the example in Fig. 2d it is clear that the slope of the projection ray is $m=-3$ which follows from (8) for $N=8$ and $a=1$. It can be noticed that for $a=1$, projection line $l=r_1$ intersects only one lattice point in the 1st octant, that is $p_3(a)=(N/2-1, N/2-1)$. This is not the case for all values of a . Our main requirement that only one projection ray intersects each pixel's upper right area can be interpreted as a requirement for the projection line l connecting points $p_3(a)$ and p_1 to intersect only one lattice point. Indeed, if line l intersects more than one lattice points then the projection ray that follows l intersects the upper right area of more than one pixel in this octant. This can be clearly seen in the examples of Fig. 3b and 3d. Therefore, from all $\lfloor N/4 \rfloor$ possible values of offset a we concern only those for which point $p_3(a)$ is mutual visible from point p_1 as in the case of Fig. 3a and 3c.

Typically, two lattice points (x_a, y_a) and (x_b, y_b) are mutually visible if the line segment joining them contains no further lattice points (Boca, 2000). Moreover, they satisfy the relation $\gcd(x_b - x_a, y_b - y_a) = 1$, where $\gcd(a, b)$ denotes the greatest common divisor of a and b . In our case this corresponds to

$$\gcd(p_{1,x} - p_{3,x}, p_{1,y} - p_{3,y}) = \gcd(a, a - N/2) = \gcd(a, N/2) = 1 \quad (11)$$

This is an important relation in our method since it states that $p_3(a)$ and p_1 are mutually visible if offset a is coprime to $N/2$. Let F_N denote the set of all values of a for which the above relation holds, that is

$$F_N = \{a : a \leq \lfloor N/4 \rfloor \text{ and } \gcd(a, N/2) = 1\} \quad (12)$$

The cardinality K_a of F_N is given by the Euler function $\varphi(n)$. Function $\varphi(n)$, also known as totient function (Finch, 2003), is defined as the number of positive integers less than or equal to n that are relatively prime to n , that is

$$\varphi(n) = \#\{a \in \mathbf{N} : a \leq n \text{ and } \gcd(a, n) = 1\} \quad (13)$$

where 1 is counted as being relatively prime to all numbers. For a prime p it is $\varphi(p) = p - 1$ since all numbers less than p are relatively prime to p . Since $a \leq \lfloor N/4 \rfloor$ the overall number of proper offset values is

$$K_a = \frac{\varphi(N/2)}{2} \quad (14)$$

Indeed, for $N=16$, it is $F_N = \{1, 3\}$, $K_a = 2$ and (8) gives $m = -7/1$ and $m = -5/3$ as shown in Fig. 3a and 3c.

Summarizing, if the image is projected on a projection axis at angle u given by (9) for $a \in F_N$ then each projection ray does not intersect the upper right area of more than one pixel in the 1st octant.

3.2 Determination of the other Projection Parameters

The width d of the projection ray is given by the width of the broadest projection ray that does not contain any lattice points of the 1st octant in its interior. Indeed, if one or more lattice points are contained in the projection ray then the upper right area of more than one pixels are intersected by this specific projection ray, which contradicts our main hypothesis. It can be shown that, if the projection lines have a direction $\tan\theta = m = a/b$, with $\gcd(a, b) = 1$ then there are projection ray paths of width $d > 0$ containing no lattice points (Olds, 2001). The width of the broadest such ray is

$$d = \frac{|ap + bq|}{\sqrt{a^2 + b^2}} = \frac{\gcd(a, b)}{\sqrt{a^2 + b^2}} = \frac{1}{\sqrt{a^2 + b^2}} \quad (15)$$

We have already defined point $p_3(a)$ as a lattice point in the diagonal with offset a from point $(N/2, N/2)$. Hence $b = N/2 - a$ and the above equation results to

$$d = \frac{2}{\sqrt{N^2 - 4aN + 8a^2}} \quad (16)$$

This equation provides the width of each projection ray (and consequently the width of the samples on the projection axis) as a function of offset a . According to Fig. 4 the area of the triangle that forms the intersection between a projection ray and the upper right area of a pixel equals

$$w = \frac{(ML)(KL)}{2} = \frac{d^2}{2 \sin u \cos u} = \frac{d^2}{\sin 2u} \quad (17)$$

Using equations (9) and (16) this can be written as a function if a as

$$w = \frac{4}{(N^2 - 4aN + 8a^2) \sin\left(2 \arctan\left(\frac{2a}{N - 2a}\right)\right)} = \frac{1}{(N - 2a)a} \quad (18)$$

The intersection area $w_{\theta,s}(i, j)$ between any pixel (i, j) and a projection ray perpendicular to angle θ_k and displacement s can be calculated as a multiple of w . Indeed, as shown in Fig. 4, any intersection area can be constructed as a sum of one or more right triangles of area w . For a projection axis at angle $\tan(\theta) = a/b$, where a, b are coprime numbers with $a < b$ and $b \neq 0$, the displacement k inside the pixel's area is

$$k = \begin{cases} s - s_c & \text{if } s_c \leq s \leq s_f \\ 0 & \text{otherwise} \end{cases} \quad (19)$$

with $s_c = aj + bi$ and $s_f = s_c + K_p - 1$. The number of triangles inside the projection area is given by

$$m(k) = \begin{cases} 2k + 1 & \text{if } 0 \leq k < a \\ 2a & \text{if } a \leq k < b \\ 2(K_p - k) - 1 & \text{if } b \leq k \leq K_p - 1 \end{cases} \quad (20)$$

Hence, the intersection area in the k -th displacement is

$$w_{\theta,s}(i, j) = m(k)w \quad (21)$$

Equation (18) implies also that for given image dimension N , the area w is maximum for $a=1$ and decreases as a reaches $\lfloor N/4 \rfloor$. Regarding the parameters K_p and K_l it follows from Fig. 4 that

$$K_p = \frac{(CF)}{d} = \frac{\cos(u) + \sin(u)}{d} = \frac{N}{2} \quad (22)$$

and

$$K_l = NK_p = \frac{N^2}{2} \quad (23)$$

These relations are in accordance with (3) and show that the number of projection ray intersecting each pixel as well as the overall number of samples in the projection axis do not dependent on offset a .

3.3 Image Reconstruction

The reconstruction methodology described in section 2.3 can be applied for any value of $a \in F_N$. Indeed, equations (9), (16) and (18) provide the view angle u , the width of the projection ray d and the intersection area w as a relation of image dimension N and offset a . Thus, if the original image is projected onto four projection axes whose parameters are defined by these relations then the original image pixels can be recovered from accumulator array C . The process described in section 2.3 can be considered as a special utilization using parameter settings calculated for $a=1$. However there is a significant difference concerning the decomposition sequence. In section 2.3 sequence $T_1\{t\}$ is defined by the pixels of the 1st octant sorted column-wise from the periphery to the inner of the image. In its general form, the decomposition sequence $T_a\{t\}$ holds the pixels of the 1st octant sorted decreasingly according to their s_f value, that is the furthest from the origin projection ray that intersects each pixel. Fig. 5 depicts two decomposition sequences for $N=16$. On the left example, it is $a=1$ while on the right example, the offset is $a=3$ resulting to a different re-ordering of the pixels in the decomposition sequence.

Fig. 6 depicts the reconstruction of the well known phantom image (Shepp, 1974) of size $N \times N = 256 \times 256$ pixels using three different view angles. The image is projected into four projection axes given by (2) which are symmetrically oriented with respect to the horizontal and vertical axis, as shown in Fig. 1. In all the cases the pixels in the periphery of the image are reconstructed first followed by the pixels in the center of the image. For each pixel in the decomposition sequence its

symmetrical pixels in the other octants are also reconstructed leading to a symmetrical outer-to-inner reconstruction of the image. However, the order in which the pixels are considered depends on the view angle u which, in turn, is directly related to the applied offset value. In the left column of Fig. 6 the image is reconstructed using an offset value $a=1$ which corresponds to a view angle $u=0.45^\circ$. It can be clearly seen that pixels are reconstructed column-wise or row-wise, depending on the octant in which the process is applied. In the middle and the right column the offset values are $a=23$ and $a=63$, corresponding to view angles $u=12.36^\circ$ and $u=44.10^\circ$, respectively. The later is the highest value of a that can be used for the given image dimensions according to (12). Clearly, there is a different decomposition sequence for any of the K_a available values of a , but all of them lead finally to the exact reconstruction of the original image. It should be also noticed, that if $N=2p$ where p a prime number then according to (14) there is a maximum of

$$K_a = (p-1)/2 = (N-2)/4 \quad (24)$$

available offset values and consequently $(N-2)/4$ different view angles u according to which the four projection axes can be oriented.

3.4 Complexity and Applicability

Let $n=N^2$ denote the overall number of pixels in the image. The memory requirements of the proposed methods is $O(n)$. Indeed, the accumulator array requires $K_\theta K_f = 4(n/2) = 2n$ memory units and there are $n/8$ entries in decomposition sequence $T_a\{t\}$. Considering time complexity, the most consuming processes are the decomposition sequence determination and the reconstruction process. Although sorting the pixels during the determination of $T_a\{t\}$ is $O(n^2)$ in the worst case, the average time is $O(n \log n)$ (Havil, 2003). The complexity for the reconstruction process is related to the decomposition of the accumulator array C which is $O(n\sqrt{n})$. It should be noticed that $T_a\{t\}$ is not related to the image's contents. Therefore, it is not necessary to determine the decomposition sequence each time an $N \times N$ image is considered. Instead, it can be determined once for a given set of parameter settings N and a_k and then retrieved from a lookup table anytime an image with the same parameters is considered.

4 CONCLUSIONS

In this paper we presented a sequential reconstruction method that allows the exact reconstruction of an image when it is projected into four projection axes which are symmetrically oriented with respect to the horizontal and the vertical axis at coprime ratio view angles. Analytical relations are provided that determine the parameter settings, namely the set of proper view angles, the density of samples in each projection axis and the intersection area between a pixel and a projection ray. The chosen view angle affects the decomposition sequence which determines the order in which the pixels are restored. The image is reconstructed by a one pass decomposition process where the external pixels are restored first followed by the pixels in the image's center. It should be noticed that we addressed the proposed method as a quantitative reconstruction process problem and did not consider optimization of noise propagation. Future work includes a detailed analysis of the algorithm's behavior when noisy data are present as well as the formulation of the proposed method in an increasingly detailed hierarchical reconstruction approach.

REFERENCES

Boca, F. P., Cobeli, C, Zaharescu, A. , 2000. Distribution of Lattice Points Visible from the Origin. In *Comm. Math. Phys.*, vol 213, pp. 433-470.

Clackdoyle, R., Noo, F., Guo, J., Roberts, J. A. , 2004. Quantitative reconstruction from truncated projections in classical tomography. In *IEEE Trans. Nucl. Sci.*, vol. 55(2), pp. 2570-2578.

Delaney, A. H., Bresler, Y., 1998. Globally convergent edge-preserving regularized reconstruction: an application to limited-angle tomography. In *IEEE Trans. Image Process.*, vol. 7, pp. 204-221.

Finch, S. R., 2003. Euler Totient Constants. In *Mathematical Constants*. Cambridge University Press, pp. 115-119.

Havil, J., 2003. Quicksort Gamma: Exploring Euler's Constant, Princeton University Press, pp. 128-130.

Natterer, F. , 2001 *The Mathematics of Computerized Tomography*. Philadelphia, SIAM.

Olds, C. D., Lax, A., Davidoff, G. P., 2001. *The Geometry of Numbers*, The Mathematical Association of America.

Rantala, M., Vanska, S., Jarvenpaa, S., Kalke, M., Lassas, M., Moberg, J. Siltanen, S., 2006. Wavelet-based reconstruction for limited-angle X-ray tomography. In *IEEE Trans. Med. Imag.*, vol 25 (2), pp. 210-217.

Schule, T., Weber, S., Schnorr, C., 2005. Adaptive Reconstruction of Discrete-Valued Objects from few Projections. In *Electronic Notes in Discrete Mathematics*, vol. 20, pp. 365-384.

Shepp, L. A., Logan, B. F., 1974. The Fourier reconstruction of a head section. In *IEEE Trans. Nucl. Sci.*, vol. 21, pp. 21-43.

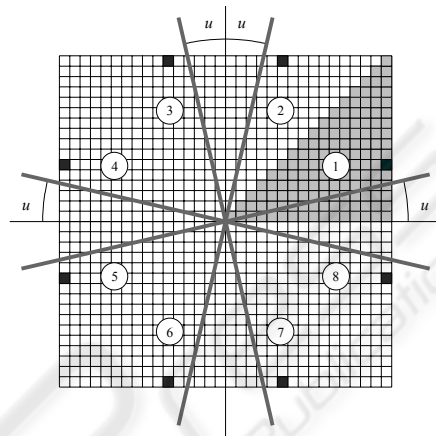


Figure 1: The image is divided into eight octants. The gray shaded pixels denote the 1st octant. The black pixels denote pixels with symmetrical geometric properties.

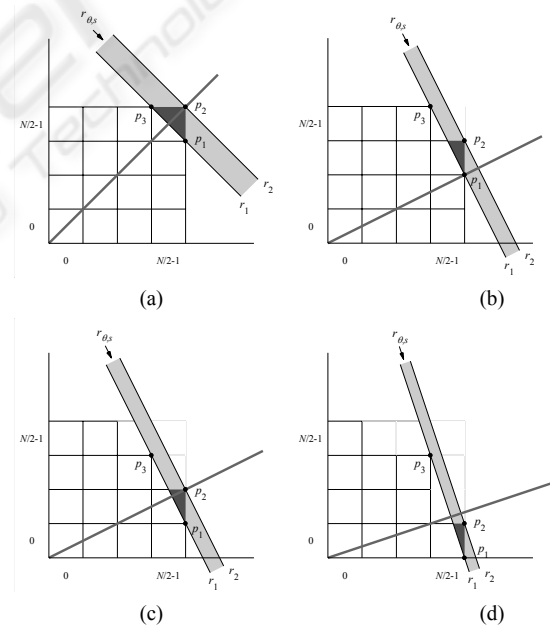


Figure 2: Intersection of a projection ray and the pixel $(i, i-n)$ in the 1st octant of an $N \times N = 8 \times 8$ pixels image. Four cases are shown where $i = N/2 - 1$ and $n = 0, 1, 2$ and 3 , respectively. In each case the light shaded strip depicts the projection ray and the dark shaded area denotes the intersection between the pixel and the projection ray.

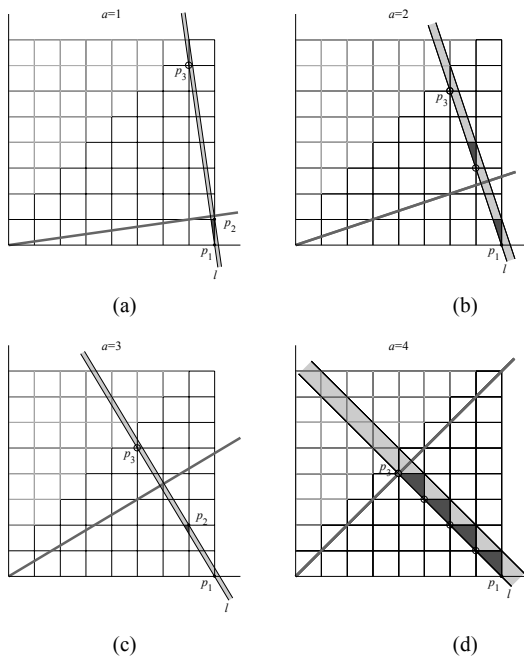


Figure 3: The number of pixels whose upper right area is intersected by a projection line equals the number of lattice points of the 1st octant joining the line segment l between $p_3(a)$ and p_1 (denoted by a circle). There is a unique such pixel if offset a is coprime to $N/2$ (subfigures (a) and (c)), and more than one, otherwise (subfigures (b) and (d)). In any case the dark shaded area denotes the intersection between the upper right area of a pixel and the projection ray.

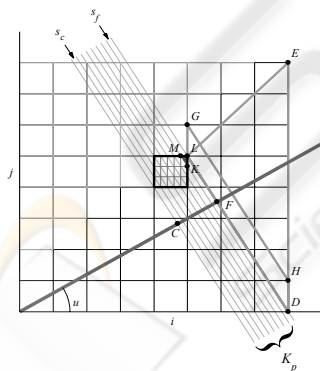


Figure 4: Each pixel is intersected by K_p projection rays. The dark shaded area denotes the intersection between pixel (i, j) and the projection ray s_f that is the furthest from the origin ray that intersects the pixel.

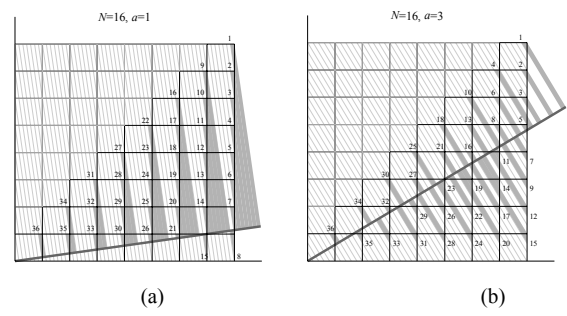


Figure 5: Decomposition sequence $T_a\{t\}$ of an $N \times N = 16 \times 16$ sized image for (a) $a=1$ and (b) $a=3$. In each case the pixels are sorted according to the furthest from the origin projection ray that intersects them.

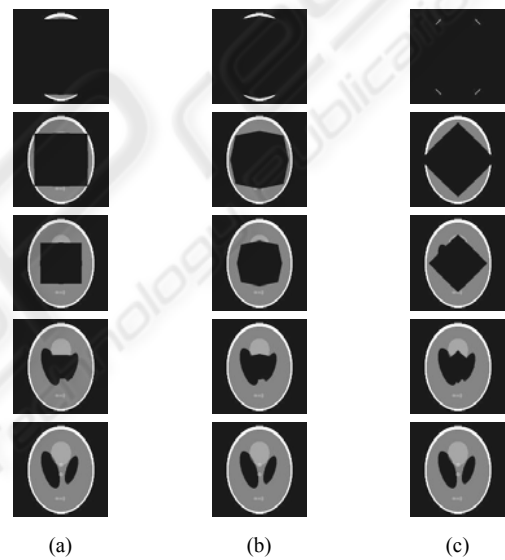


Figure 6: Reconstruction of a 256×256 phantom image using three different projection angles. The offset values are (a) $a=1$, (b) $a=23$ and (c) $a=63$. In each case, the symmetrical orientation of the four projection axes around the horizontal and the vertical axis result to an outer-to-inner reconstruction of the image.